ADAPTIVE SPACE FRAME ANALYSIS: PART II, A DISTRIBUTED PLASTICITY APPROACH

B.A. IZZUDDIN[‡] AND A.S. ELNASHAI[#]

1. ABSTRACT

In a previous companion paper (Part I: A Plastic Hinge Approach), adaptive elasto-plastic analysis of space frames was discussed in the context of a plastic hinge approach. The present paper extends the concept of automatic mesh refinement to deal with accurate elasto-plastic large displacement analysis accounting for the spread of yield within structural members. This is achieved through the use of the quartic formulation in the elastic range, and performing automatic subdivision of quartic elements into elasto-plastic cubic elements which account for the spread of plasticity across the section depth and along the element length. The main advantage of this approach is the ability to start full elasto-plastic large displacement analysis using only one element per member, with automatic mesh refinement performed only where and when necessary within the structure and during the analysis. The paper presents a description of the elasto-plastic cubic formulation, discusses the concept of automatic mesh refinement in the context of elasto-plastic analysis, and provides verification examples using the computer program ADAPTIC to demonstrate the accuracy and extreme efficiency of the proposed nonlinear analysis procedure.

2. INTRODUCTION

Two main approaches for the large displacement elasto-plastic analysis of framed structures were identified in the companion paper[1]; namely, the plastic hinge and the distributed plasticity approaches. Whilst the computational advantage of plastic hinge analysis is significant, such an approach is only suitable for preliminary approximate analysis, since it is unable to deal with the spread of plasticity. Moreover, the modelling of realistic stress-strain laws in the context of the

[‡] Lecturer in Computing, Civil Engineering Dept., Imperial College, London, UK.
[#] Reader in Earthquake Engineering, Civil Engineering Dept., Imperial College, London, UK.

plastic hinge approach is sufficiently complex, which often leads to the simplifying assumption of elastic-perfectly plastic material. The previous paper[1] discussed plastic hinge analysis in the large displacement domain, and outlined in that context a procedure for automatic mesh refinement deemed essential for modelling elasto-plastic beam-column buckling.

The present paper focuses on elasto-plastic analysis of framed structures accounting for the spread of plasticity across the section depth and along the member length. Moreover, primary consideration is given to the attainment of accurate results with a minimum of computational effort. The two main factors involved are the significant computational demand posed by finite element formulations accounting for the spread of plasticity, and the need to use a number of such elements within an elasto-plastic member for accurate modelling. Within a traditional approach, elasto-plastic analysis of frames requires the use of a fine mesh of elements for all members of the structure from the start of analysis, since the locations of plasticity are not known a priori. The thesis of this paper is that the use of automatic mesh refinement in the context of elasto-plastic analysis not only provides very significant computational savings, but also maintains the original accuracy of an initially refined mesh.

The paper proceeds with a description of a fibre-type elasto-plastic cubic formulation, which accounts for the spread of plasticity within the element, and models the effect of large displacements in 2D and 3D space. The process of automatic mesh refinement is then discussed, and its computational and modelling advantages are highlighted. Finally, a number of verification examples are presented, and comparisons are made with other approaches to demonstrate the computational savings and accuracy of the proposed adaptive nonlinear analysis method.

3. ELASTO-PLASTIC CUBIC FORMULATION

As for the plastic hinge quartic formulation[1], the elasto-plastic cubic formulation is derived in a convected (Eulerian) system, where the element local displacements are referred to the element chord in its deflected state. The effect of large displacements is thus included in a similar manner, as discussed by Izzuddin and Elnashai[2]. The cubic formulation is capable of modelling material

nonlinearity effects through a detailed consideration of the section shape and the material stress-strain law, as discussed hereafter.

3.1. Kinematics

Six local degrees of freedom are employed for the 3D cubic formulation, as shown in Figure 1:

$$\left.\begin{aligned} {}_{c}\underline{u} &= \left\langle \theta_{1y}, \theta_{1z}, \theta_{2y}, \theta_{2z}, \Delta, \theta_{T} \right\rangle^{T} \\ {}_{c}\underline{f} &= \left\langle M_{1y}, M_{1z}, M_{2y}, M_{2z}, F, M_{T} \right\rangle^{T} \end{aligned}\right\} \tag{1}$$

No variables for imperfections are included in this formulation, since it is intended to represent short lengths of members, and can hence be assumed straight. The movement of a point along the element reference axis can be described by four displacement values (α,u,v,w), as shown in Figure 2, and are defined by interpolation functions given by:

$$\left.\begin{aligned} \alpha(x) &= \theta_{T}\left(\frac{x}{L}\right) \\ v(x) &= \left(\frac{\theta_{1y} + \theta_{2y}}{L^{2}}\right)x^{3} - \left(\frac{2\theta_{1y} + \theta_{2y}}{L}\right)x^{2} + \left(\theta_{1y}\right)x \\ w(x) &= \left(\frac{\theta_{1z} + \theta_{2z}}{L^{2}}\right)x^{3} - \left(\frac{2\theta_{1z} + \theta_{2z}}{L}\right)x^{2} + \left(\theta_{1z}\right)x \end{aligned}\right\} \tag{2}$$

No interpolation function is needed for the axial displacement (u), since the constant centroidal axial strain criterion is used, as discussed hereafter.

3.2. Generalized strains

In the derivation of the cubic formulation, the following assumptions are made:

1. Warping strains due to non-uniform torsion are negligible.
2. Plane sections remain plane after bending deformation.
3. Shear strains due to flexure are negligible.
4. The section centroid and shear centre are coincident and their loci represent the element reference axis.

This allows the strain state within a cross-section to be solely determined by a set of four generalized strains: centroidal axial strain, rate of twist, and curvature strains about the two principal axes.

The derivation of the centroidal axial strain includes the effect of bowing on stretching, and hence the cubic formulation is capable of modelling the beam-column effect. The centroidal axial strain is assumed constant along the element length; therefore, an interpolation function for the axial displacement (u) is not required. Although in the presence of material plasticity, this condition does not necessarily imply a constant axial force along the element length, the variation of the axial force is insignificant if the element is used to model short lengths of elasto-plastic members. The remaining three generalized strains are obtained from the assumption of small local deformation, as given below,

$$\left.\begin{aligned} \varepsilon_c &= \frac{\Delta}{L} + \frac{1}{L}\int_0^L \left(\frac{1}{2}\left\{\left(\frac{dv}{dx}\right)^2 + \left(\frac{dw}{dx}\right)^2\right\}\right) dx \\ \kappa_y &= \frac{d^2v}{dx^2} \quad , \quad \kappa_z = \frac{d^2w}{dx^2} \quad , \quad \zeta = \frac{d\alpha}{dx} \end{aligned}\right\} \tag{3}$$

where, ε_c, ζ, κ_y and κ_z represent the centroidal axial strain, the rate of twist and the curvatures about the two principal axes respectively. The combination of eqs. (2) and (3) leads to the relationship between the generalized strains and the element freedoms:

$$\varepsilon_c = \frac{\Delta}{L} + \frac{\left\{2\left(\theta_{1y}^2 + \theta_{2y}^2 + \theta_{1z}^2 + \theta_{2z}^2\right) - \left(\theta_{1y}\theta_{2y} + \theta_{1z}\theta_{2z}\right)\right\}}{30} \tag{4.a}$$

$$\kappa_y = \left(\frac{6\left(\theta_{2y} + \theta_{1y}\right)}{L^2}\right)x - \left(\frac{2\left(2\theta_{1y} + \theta_{2y}\right)}{L}\right) \tag{4.b}$$

$$\kappa_z = \left(\frac{6\left(\theta_{2z} + \theta_{1z}\right)}{L^2}\right)x - \left(\frac{2\left(2\theta_{1z} + \theta_{2z}\right)}{L}\right) \tag{4.c}$$

$$\zeta = \frac{\theta_T}{L} \tag{4.d}$$

Since the relationship between the generalized stresses and strains cannot be established explicitly in the presence of material plasticity, the integration of the virtual work equation to obtain the element

forces is performed numerically. Only two Gauss integration sections are employed along the length, again because the element can only represent short lengths of members. The position of the Gauss sections, shown in Figure 3, is chosen such that exact integration of the virtual work equation is obtained for the elastic element:

$$\left.\begin{aligned} {}^{g}x_{1} &= \frac{L}{2}\left(1 - \frac{\sqrt{3}}{3}\right) \\ {}^{g}x_{2} &= \frac{L}{2}\left(1 + \frac{\sqrt{3}}{3}\right) \end{aligned}\right\} \tag{5}$$

The generalized strains at both Gauss sections are, hence, represented by a matrix ${}^{s}u$:

$${}^{s}u = \begin{bmatrix} \varepsilon_c & \varepsilon_c \\ \kappa_y\left({}^{g}x_{1}\right) & \kappa_y\left({}^{g}x_{2}\right) \\ \kappa_z\left({}^{g}x_{1}\right) & \kappa_z\left({}^{g}x_{2}\right) \\ \zeta & \zeta \end{bmatrix} \tag{6}$$

which can be explicitly determined from eqs. (4) and (5).

3.3. Generalised stresses

Each Gauss section is divided into a number of areas across which strains and stresses are monitored, as shown in Figure 4 for certain cross-sectional configurations. If the effect of shear strains on material plasticity is neglected, only direct strains need to be established at the monitoring points:

$$e_{m,g} = \sum_{i=1}^{4} d_{m,i}\ {}^{s}u_{i,g} \tag{7}$$

where ${}^{e}{}_{m,g}$ is the direct strain of monitoring point 'm' at Gauss section 'g',

$$\left.\begin{aligned} d_{m,1} &= 1 \\ d_{m,2} &= -y_m \\ d_{m,3} &= -z_m \\ d_{m,4} &= 0 \end{aligned}\right\} \tag{8}$$

and ${}^{s}u$ is the generalized strain matrix defined in eq. (6).

A uniaxial stress-strain relationship is employed to establish the direct stresses at the monitoring points:

$$s_{m,g} = \sigma(e_{m,g}) \tag{9}$$

in which "σ" can represent any stress-strain law, as demonstrated by Elnashai and Izzuddin[3].

For the element tangent stiffness calculation needed for the iterative solution procedure, a material tangent modulus is required:

$$tE_{m,g} = \frac{d\, s_{m,g}}{d\, e_{m,g}} = \frac{d\, \sigma}{d\, \varepsilon}(e_{m,g}) \tag{10}$$

The bending and axial generalized stresses at a Gauss section are determined from the material direct stresses, while the relation between the torsion generalized strain and stress is based on the elastic rigidity constant:

$$\left.\begin{aligned} sf_{i,g} &= \sum_{m=1}^{n} A_m\, d_{m,i}\, s_{m,g} \qquad \text{for } i = 1, 3 \\ sf_{4,g} &= GJ\, su_{4,g} \end{aligned}\right\} \tag{11}$$

where A_m is the area of monitoring point 'm', $d_{m,i}$ is defined in eq. (8), and 'n' is the number of monitoring points at a Gauss section.

3.4. Local forces and stiffness

After the generalized stresses are obtained at the two Gauss sections, the element local forces can be established from numerical integration of the virtual work equation[4]:

$$cf_i = \sum_{j=1}^{4} \sum_{g=1}^{2} cT_{i,j,g}\, sf_{j,g} \tag{12}$$

where cT is a 6x4x2 matrix representing weighted first derivatives of generalised strains with respect to local displacements, and which is given in Appendix A.

The local tangent stiffness ck is obtained through differentiation of eq. (12), and can be expressed as[4]:

$$ {}_{c}k_{i,k} = {}_{f}k_{i,k} + \left(\frac{2}{L}\right) \sum_{j=1}^{4} \sum_{g=1}^{2} \sum_{h=1}^{4} {}_{c}T_{i,j,g} \; {}_{s}k_{j,h,g} \; {}_{c}T_{k,h,g} \qquad (13) $$

in which ${}_{f}k$ and ${}_{s}k$ are determined according to the following,

$$ \left.\begin{array}{l} {}_{f}k_{1,1} = {}_{f}k_{2,2} = {}_{f}k_{3,3} = {}_{f}k_{4,4} = \dfrac{2\,FL}{15} \\ {}_{f}k_{1,2} = {}_{f}k_{2,1} = {}_{f}k_{3,4} = {}_{f}k_{4,3} = -\dfrac{FL}{30} \\ \text{'F' is the axial force, and all other terms are zero} \end{array}\right\} \qquad (14) $$

and,

$$ \left.\begin{array}{l} {}_{s}k_{j,h,g} = \sum_{m=1}^{n} A_m \, d_{m,j} \, {}_{t}E_{m,g} \, d_{m,h} \qquad \text{for } j = 1, 3 \;\&\; h = 1, 3 \\ {}_{s}k_{4,4,g} = GJ \\ \text{All other terms are zero} \end{array}\right\} \qquad (15) $$

where ${}_{t}E$ is defined in eq. (10).

3.5. Global analysis

Global structural analysis including geometric nonlinearity effects is performed for the cubic formulation in an identical manner as for the plastic hinge quartic formulation[1]. In the calculation of direct stresses at the monitoring points according to eq. (9), strains must be considered incrementally from the last equilibrium state. This requires storage of material variables (stresses, strains, etc..) at the start of the load increment and for the current iteration, with the variables of the former updated only after global equilibrium is achieved.

4. ADAPTIVE MESH REFINEMENT

The elasto-plastic cubic formulation, discussed in the previous section, is capable of modelling the spread of plasticity across the section and along the element, by virtue of the use of monitoring areas

for stresses and strains at the two Gauss sections. The computational demand of the cubic formulation is significant, especially for complicated stress-strain relationships, since the stress-strain response has to be monitored for an often large number of monitoring areas to achieve accurate representation of the plasticity spread within the section. Moreover, the accurate modelling of the spread of plasticity along the member requires the use of a number of cubic elements, since a cubic shape function for the transverse displacements and the constant centroidal axial strain criterion do not qualify the formulation to represent a whole elasto-plastic member. In the context of a traditional modelling approach, a fine mesh of elasto-plastic elements is required for all members of the structure, since the locations of plasticity within the structure are not known before analysis. This leads to a considerable computational demand, rendering the use of the distributed plasticity approach impractical for most realistic structures.

The concept of automatic mesh refinement, discussed in the companion paper[1] for the plastic hinge approach, is extended herein to deal with the above inefficiencies pertinent to traditional distributed plasticity modelling. The proposed procedure relies on the accuracy of the quartic formulation[4] in representing imperfect elastic beam-columns using only one element per member, and the ability of the cubic formulation to model the spread of plasticity within elasto-plastic members using a number of elements. At the start of analysis, a member is modelled by one elastic quartic element. In the course of load incrementation, yield is checked at the extreme fibres of selected sections along the element length. If yield is detected, elasto-plastic cubic elements are inserted only in the zones of plasticity, while the rest of the element is re-modelled with elastic quartic elements, before the analysis is continued.

The main advantage of the automatic mesh refinement process is the significant computational savings, since the computer-intensive elasto-plastic cubic elements are introduced only *where* required within the structure, and *when* necessary during analysis. Moreover, the modelling advantages are considerable, since the meshing of the structure at the start of analysis can be performed using only one element per member. The main components of the automatic mesh refinement procedure are described hereafter.

4.1. Yield check

The check for yield along the length of the quartic element is performed for each load step at selected sections. These sections correspond to the Gauss integration positions of the cubic elements to be inserted if yield is detected, with the configuration of the refined mesh specified before analysis, as shown in Figure 5.

The biaxial moments at a section are calculated in the same manner as for the plastic hinge approach, discussed in the companion paper[1]. If the combination of the axial force and bending moments at a section results in yielding at the extreme fibres, then a cubic element is inserted at the corresponding location, while the elastic parts are kept as quartic elements. If none of the sections have yielded, then mesh refinement is not performed.

The current load step must be re-applied if any of the structure quartic elements has been subjected to mesh refinement; otherwise, the analysis proceeds to the next load step.

Elastic quartic elements which are the result of an earlier mesh refinement process are checked for yield at sections corresponding to the remaining elastic parts of the original element. Thus, after a mesh refinement process, information must be passed to identify for the new elastic quartic elements the sections at which yielding is to be checked as the analysis proceeds.

4.2. Mesh refinement

Within the distributed plasticity approach, mesh refinement involves the creation of a number of new nodes, new elasto-plastic cubic elements and new elastic quartic elements, as shown in Figure 6.

As with the plastic hinge approach[1], the global displacements of the new nodes are established at the last equilibrium configuration from the deflected shape of the original element and the global displacements of its end nodes.

For the new elements, variables corresponding to the initial and last equilibrium configurations must be determined. For the cubic elements, these include initial direction cosines, orientation of the principal axes at both ends, local displacements, stresses and strains at monitoring points, and local forces. While for the quartic elements they include initial direction cosines, initial imperfections, orientation of the principal axes at both ends, local displacements, local forces, and mesh refinement

configuration. Similar to the plastic hinge approach, allowance must be made for the nonlinear variation of the axial displacement along the original element length, which is due to the effect of bowing on axial stretching.

5. VERIFICATION EXAMPLES

The methodology for accurate elasto-plastic large displacement analysis of space frames, discussed previously, has been implemented in ADAPTIC[5], in coexistence with the plastic hinge approach. Three examples are presented herein to demonstrate the accuracy of the proposed distributed plasticity approach and the significant computational savings achieved using the concept of automatic mesh refinement in the context of elasto-plastic analysis. All reported CPU times are for ADAPTIC v2.1.2, running on a Silicon Graphics workstation with 24 Mb of physical memory and rated at 30 mips, 4.2 mflops and 26 Specmarks.

5.1. K-frame

In this example, comparison is made between the prediction of ADAPTIC, using the plastic hinge and distributed plasticity approaches, and the analytical and experimental results reported by Soreide et al[6] on the K-frame set-up shown in Figure 7. Although Soreide et al did not include any information regarding the level of imperfections, it was found that ADAPTIC provides best comparison with the experimental ultimate capacity if parabolic imperfections of (L/1000) are assumed in the diagonal members.

Soreide et al used the computer program USFOS, which employs a beam-column formulation with sinusoidal or hyperbolic shape functions, and adopts the plastic hinge approach to model the effect of yielding. The comparison with experimental results in Figure 8. shows that the prediction of USFOS overestimates the ultimate capacity by 17%, while underestimating the response in the post-buckling range.

With ADAPTIC, the plastic hinge approach with automatic mesh refinement is first used[1]. The analysis is started using four plastic hinge quartic elements, whereupon detection of a plastic hinge within either of the diagonal elements, automatic sub-division into two elements is performed, as

shown in Figure 9. With this approach, the ultimate capacity is overestimated by 9%, compared to the 17% overestimate predicted by USFOS (Figure 8). The improved accuracy may be attributed to the occurrence of plastic hinges within the diagonal members away from mid-length, which reinforces the argument presented in the companion paper regarding the need for automatic mesh refinement to account for such a possibility.

The results of ADAPTIC are also obtained using the distributed plasticity approach, where the analysis is started with four quartic elastic elements, and automatic mesh refinement into elasto-plastic cubic elements is performed upon detection of yield. By the end of analysis, 32 cubic elements, employing the bilinear kinematic material model with a strain hardening parameter of 0.1%, are inserted in the yielding zones, while the rest of the frame is still modelled by elastic quartic elements, as shown in Figure 10. This approach provides more favourable comparison with the experimental results in terms of ultimate capacity (0.2% overestimate) and post-buckling response prediction, as demonstrated in Figure 8.

This example demonstrates the high levels of accuracy that can be achieved with the distributed plasticity approach, although, it may be argued, that the plastic hinge approach is sufficiently accurate. The issue of accuracy versus efficiency of the two approaches can be highlighted by considering the CPU times, where the distributed plasticity approach requires 42.3 seconds while the plastic hinge approach requires only 8.2 seconds. However, no general conclusions can be made regarding the relative merits of the two approaches, since the problem considered in this example is reasonably small, and the material stress-strain relationship is almost elastic-plastic without strain-hardening. For realistic problems, the efficiency of the plastic hinge approach may not be so pronounced, as shown in the last example, in which case accuracy considerations play an important role in choosing the appropriate approach.

5.2. One-bay steel jacket

The steel jacket structure, shown in Figure 11, is subjected to a transient seismic signal having a duration of 4 seconds (see Figure 12). The aim of this example is to demonstrate the considerable efficiency of the proposed automatic mesh refinement process at no loss in accuracy, and, therefore, the analysis is performed with ADAPTIC using two distributed plasticity approaches. The first uses

an initially refined mesh of 400 elasto-plastic cubic elements, with 8 elements modelling each of the braces and 6 elements used for the rest of the members. Whereas the second approach starts with only 52 elastic quartic elements and employs the automatic mesh refinement process to model the elasto-plastic behaviour, potentially subdividing the original mesh into the same 400 cubic elements if all the structural members undergo plastic deformation.

A comparison of the results from the two approaches in Figure 13 demonstrates excellent agreement, and verifies that there is no loss of accuracy resulting from the use of automatic mesh refinement. However, automatic mesh refinement provides significant computational savings due to the restriction of plasticity to the jacket braces (see Figure 14), hence only 104 elasto-plastic elements are required and at a later stage in the analysis.

A detailed consideration of CPU consumption in Figure 15 shows that an initially refined mesh requires 2hrs 11min 6sec, while with automatic mesh refinement only 27min 45sec is needed. A great part of the savings with the latter approach is achieved in the elastic range, before signal time of 2 sec, where the structure is only modelled with 52 elastic quartic elements as opposed to 400 elasto-plastic cubic elements. However, more savings are obtained after the occurrence of plasticity, since only part of the structure undergoes plasticity and 44 elastic elements with 104 elasto-plastic elements provide accurate representation.

In general, using the automatic mesh refinement process can never be less efficient than using an initially refined mesh, since at worst all the structure members are automatically refined from the first time-step and an initially refined situation is achieved. However, the relative efficiency of the two approaches may vary depending on the time-history of the spread of plasticity within the structure. This is demonstrated in Figure 16, where automatic mesh refinement is about 20 times more efficient than an initially refined mesh in the elastic range, with that ratio dropping to about 5, still a considerable saving, after plasticity is achieved.

5.3. 3D jacket under earthquake loading

This example is a repeat of the one presented in section 7.4 of the companion paper[1], except that the distributed plasticity approach is used instead of the plastic hinge approach. The purpose of this

example is to verify the accuracy of both approaches in the nonlinear analysis of realistic structures, and to provide a comparison of accuracy and efficiency in that context.

The comparison of results in Figure 17 demonstrates only minor differences in the predictions of the two approaches, which are mainly attributed to the inability of the plastic hinge approach to account for the spread of plasticity within the cross-section and along the member. Such difference, however, could be much more significant if strain-hardening effects are included, or a realistic cyclic model for steel is employed[3]. It is also worth noting that, whilst the direction of buckling of the braces is different for the two approaches (compare Figure 18 herein to Figure 22 in the companion paper[1]), the overall response of the structure is not significantly affected. This asserts the bifurcation nature of brace buckling for the problem under consideration.

In terms of efficiency, the distributed plasticity approach requires a CPU time of 2hrs 34min 40sec whereas the plastic hinge approach requires 1hr 18min 3sec. The comparison of CPU time ratios, a ratio of 2 for this example compared to a ratio of 5 for the first example, shows that the relative efficiency of the two approaches is problem dependent, although the plastic hinge approach is generally more efficient. It also suggests that the distributed plasticity approach is not necessarily prohibitively expensive, as may be expected, and should hence always be used in situations where accuracy is important, and the assumptions of the plastic hinge approach impose severe simplifications over the problem in hand. However, it must be noted that the achieved efficiency of the distributed plasticity approach is mainly attributed to the automatic mesh refinement process proposed in this paper, as shown in the previous example.

6. CONCLUSIONS

This paper presented adaptive space frame analysis based on a distributed plasticity approach. The proposed approach is based on modelling the structure using one elastic quartic element per member at the start of analysis, and performing a process of automatic mesh refinement in which elasto-plastic cubic elements are inserted *where* and *when* needed, within the structure and during analysis, respectively. The process is therefore temporally and spatially adaptive. It was recognised that the

accuracy of the proposed methodology benefits largely from the ability of the quartic formulation to model the elastic geometrically nonlinear behaviour of an imperfect member using only one element.

The paper presented the formulation of the elasto-plastic cubic element, which employs Gaussian quadrature at two sections across which stresses and strains are monitored for a number of points. The improved accuracy of the cubic formulation in comparison with plastic hinge formulations was discussed, and was attributed to the ability of this formulation to model the spread of plasticity as well as the effect of realistic material stress-strain laws, albeit at the expense of employing a number of elements per member.

The process of automatic mesh refinement within elasto-plastic analysis was outlined, pointing out the departure from conventional finite element modelling. In this context, it was shown that the inefficiencies associated with the use of a number of elasto-plastic elements to model each and every member of the structure, since the locations of plasticity are unknown a priori, can be completely avoided. Also, the benefits that automatic mesh refinement avails in terms of ease of structural modelling, since a mesh of only one element per member is required, were mentioned.

Finally, the paper presented a number of verification examples, where comparisons were made with the results from other work and the plastic hinge approach. The accuracy of the distributed plasticity approach was shown to be superior to that of the plastic hinge approach, although, in general, it was found that the latter approach is more efficient. However, it was observed that the relative efficiency of the two approaches depends on the particular problem under consideration. It was therefore suggested that the distributed plasticity approach should be employed for cases where accuracy is important, since efficiency differences are generally not very significant. The importance of automatic mesh refinement in that context was demonstrated in one of the examples, where an improvement factor of 5 to 20 was achieved by the proposed methodology in comparison with conventional finite element modelling.

7. ACKNOWLEDGEMENTS

The authors would like to thank Professor Patrick J. Dowling for his continuous technical and moral support of this work. The assistance provided by the Edmund Davis fund of the University of London is also gratefully acknowledged.

8. REFERENCES

1. Izzuddin, B.A. and Elnashai, A.S. Adaptive space frame analysis: Part I, A plastic hinge approach. (*companion paper*), 1993.
2. Izzuddin, B.A. and Elnashai, A.S. Eulerian Formulation for large displacement analysis of space frames. J. Eng. Mech. Div., ASCE, 1993, Vol. 119, No. 3, pp. 549-569.
3. Elnashai, A.S. and Izzuddin, B.A. Modelling of material nonlinearities in steel structures subjected to transient dynamic loading. Int. J. Earthq. Eng. Struct. Dyn., 1993, Vol. 22.
4. Izzuddin, B.A. Nonlinear dynamic analysis of framed structures. Thesis submitted for the degree of Doctor of Philosophy in the University of London, Department of Civil Engineering, Imperial College, London, 1991.
5. Izzuddin, B.A. and Elnashai, A.S. ADAPTIC: A Program for the Adaptive Dynamic Analysis of Space Frames. Report No. ESEE-89/7, 1989, Imperial College, London.
6. Soreide T.H., Amdahl J., Granli T. and Astrud O.C. Collapse analysis of framed offshore structures. 18th Annual Offshore Technology Conference, Houston, Texas, 1986, pp. 95-102.

APPENDIX A MATRIX $_cT$

The matrix $_cT$ required in eq. (12) is given by:

$$ {}_cT_{i,j,g} = \left(\frac{L}{2}\right)\left(\frac{\partial_s u_{j,g}}{\partial_c u_i}\right) \tag{16.a} $$

$$ \left.\begin{aligned} {}_cT_{1,1,1} &= {}_cT_{1,1,2} = \frac{L\left(4\theta_{1y} - \theta_{2y}\right)}{60} \\ {}_cT_{1,2,1} &= -\frac{\left(1+\sqrt{3}\right)}{2} \quad , \quad {}_cT_{1,2,2} = -\frac{\left(1-\sqrt{3}\right)}{2} \\ {}_cT_{1,3,1} &= {}_cT_{1,3,2} = {}_cT_{1,4,1} = {}_cT_{1,4,2} = 0 \end{aligned}\right\} \tag{16.b} $$

$$ \left.\begin{aligned} {}_cT_{2,1,1} &= {}_cT_{2,1,2} = \frac{L\left(4\theta_{1z} - \theta_{2z}\right)}{60} \\ {}_cT_{2,2,1} &= {}_cT_{2,2,2} = {}_cT_{2,4,1} = {}_cT_{2,4,2} = 0 \\ {}_cT_{2,3,1} &= {}_cT_{1,2,1} \quad , \quad {}_cT_{2,3,2} = {}_cT_{1,2,2} \end{aligned}\right\} \tag{16.c} $$

$$ \left.\begin{aligned} {}_cT_{3,1,1} &= {}_cT_{3,1,2} = \frac{L\left(4\theta_{2y} - \theta_{1y}\right)}{60} \\ {}_cT_{3,2,1} &= -{}_cT_{1,2,2} \quad , \quad {}_cT_{3,2,2} = -{}_cT_{1,2,1} \\ {}_cT_{3,3,1} &= {}_cT_{3,3,2} = {}_cT_{3,4,1} = {}_cT_{3,4,2} = 0 \end{aligned}\right\} \tag{16.d} $$

$$ \left.\begin{aligned} {}_cT_{4,1,1} &= {}_cT_{4,1,2} = \frac{L\left(4\theta_{2z} - \theta_{1z}\right)}{60} \\ {}_cT_{4,2,1} &= {}_cT_{4,2,2} = {}_cT_{4,4,1} = {}_cT_{4,4,2} = 0 \\ {}_cT_{4,3,1} &= {}_cT_{3,2,1} \quad , \quad {}_cT_{4,3,2} = {}_cT_{3,2,2} \end{aligned}\right\} \tag{16.e} $$

$$
\left.
\begin{aligned}
&{}^{c}T_{5,1,1} = {}^{c}T_{5,1,2} = \frac{1}{2} \\
&{}^{c}T_{5,2,1} = {}^{c}T_{5,2,2} = {}^{c}T_{5,3,1} = {}^{c}T_{5,3,2} = {}^{c}T_{5,4,1} = {}^{c}T_{5,4,2} = 0
\end{aligned}
\right\} \qquad (16.f)
$$

$$
\left.
\begin{aligned}
&{}^{c}T_{6,1,1} = {}^{c}T_{6,1,2} = {}^{c}T_{6,2,1} = {}^{c}T_{6,2,2} = {}^{c}T_{6,3,1} = {}^{c}T_{6,3,2} = 0 \\
&{}^{c}T_{6,4,1} = {}^{c}T_{6,4,2} = \frac{1}{2}
\end{aligned}
\right\} \qquad (16.g)
$$

NOTATION

- Generic symbols of matrices and vectors are represented by bold font-type with left side subscripts or superscripts (e.g. ${}_{s}\mathbf{G}$, ${}^{a}_{q}\mathbf{u}$). This rule also applies to three-dimensional matrices.

- Subscripts and superscripts to the right side of the generic symbol indicate the term of the vector or matrix under consideration (e.g. ${}_{s}\mathbf{G}_{i,j,k}$, ${}^{a}_{q}\mathbf{u}_{i}$).

Operators

c	: right-side superscript, denotes current values during an incremental step.
o	: right-side superscript, denotes initial values during an incremental step.
T	: right-side superscript, transpose sign.
δ	: incremental operator for variables, vectors and matrices.
∂	: partial differentiation.
$\sum_{i}$	: summation over range variable (i).
[ ]	: encloses terms of a matrix.
$\langle\ \rangle$	: encloses terms of a row vector.
$\lvert a \rvert$	: magnitude of vector $\mathbf{a}$.
$\lvert a_{i} \rvert$	: absolute value of term $\mathbf{a}_{i}$.

Symbols

A	: matrix of areas of monitoring points.
d	: matrix of distances of monitoring points to the centroidal axis.

e : matrix of material strains.

$\underset{t}{E}$: matrix of material tangent modulii.

$\underset{c}{f}$: element basic local forces

$\langle M_{1y}, M_{1z}, M_{2y}, M_{2z}, F, M_T \rangle$

$\underset{q}{f}$: quartic element local forces

$\langle M_{1y}, M_{1z}, M_{2y}, M_{2z}, F, M_T, T_y, T_z \rangle$.

$\underset{s}{f}$: matrix of generalized stresses for cubic element.

G : elastic shear modulus.

J : St. Venant's torsion constant.

$\underset{c}{k}$: element local tangent stiffness matrix.

L : element length before deformation.

M_y : section moment in the local y direction.

M_z : section moment in the local z direction.

s : matrix of material stresses for cubic element.

$_cT$: matrix for transformation of generalized stresses to local forc e s .

$\underset{c}{u}$: element basic local displacements

$\langle \theta_{1y}, \theta_{1z}, \theta_{2y}, \theta_{2z}, \Delta, \theta_T \rangle$

$\underset{s}{u}$: matrix of generalized strains of cubic element.

$u(x)$: centroidal axial displacement.

$v(x)$: centroidal displacement in the local y direction.

$v^i(x)$: imperfection shape in local y direction for quartic element.

$w(x)$: centroidal displacement in the local z direction.

$w^i(x)$: imperfection shape in local y direction for quartic element.

x : reference abscissa along the element chord.

$\alpha(x)$: element twist.

ε : material strain.

ε_c : centroidal axial strain.

ζ : rate of twist.

κ_y : curvature in the local y direction.

κ_z : curvature in the local z direction.

σ : material stress.

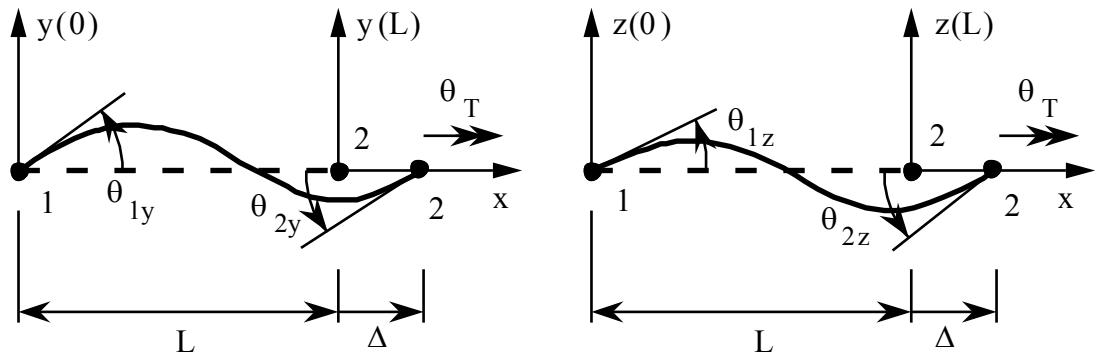


Figure 1. Local freedoms of the cubic formulation

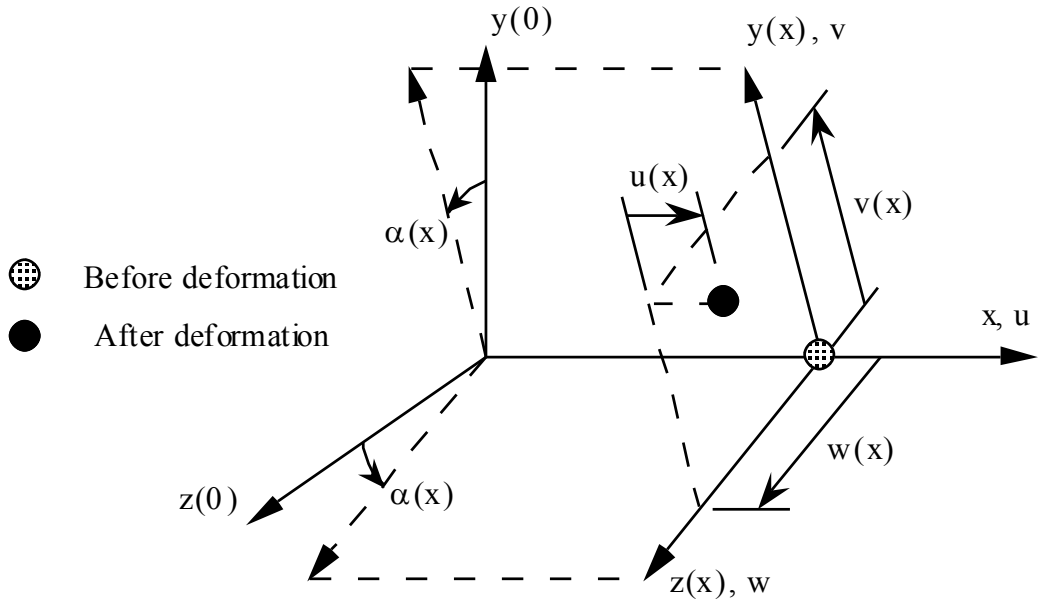


Figure 2. Movement of a reference point along the element length

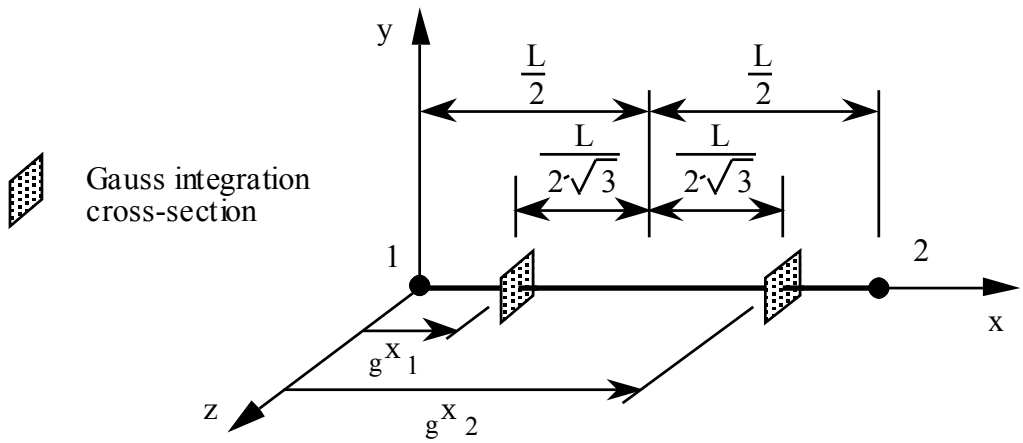


Figure 3. Location of the two Gauss integration sections

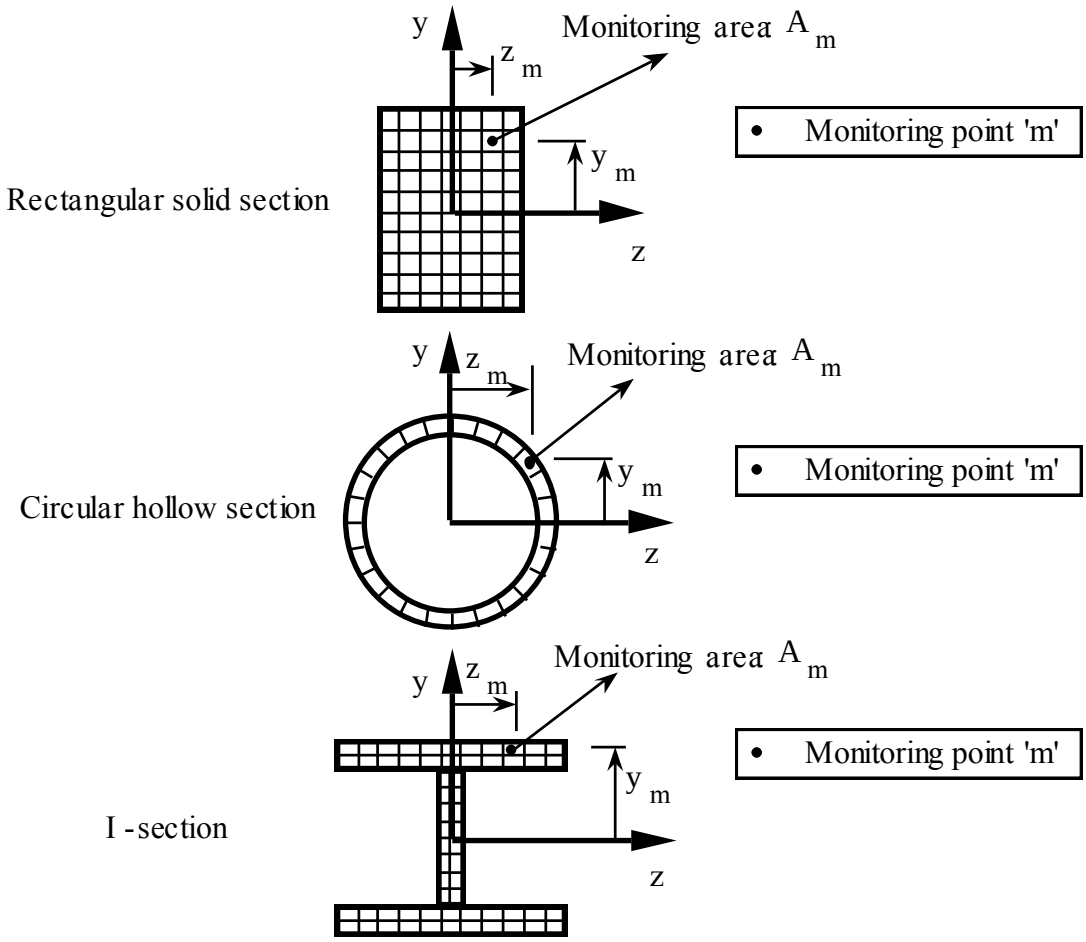


Figure 4. Distribution of monitoring points for different cross-sections

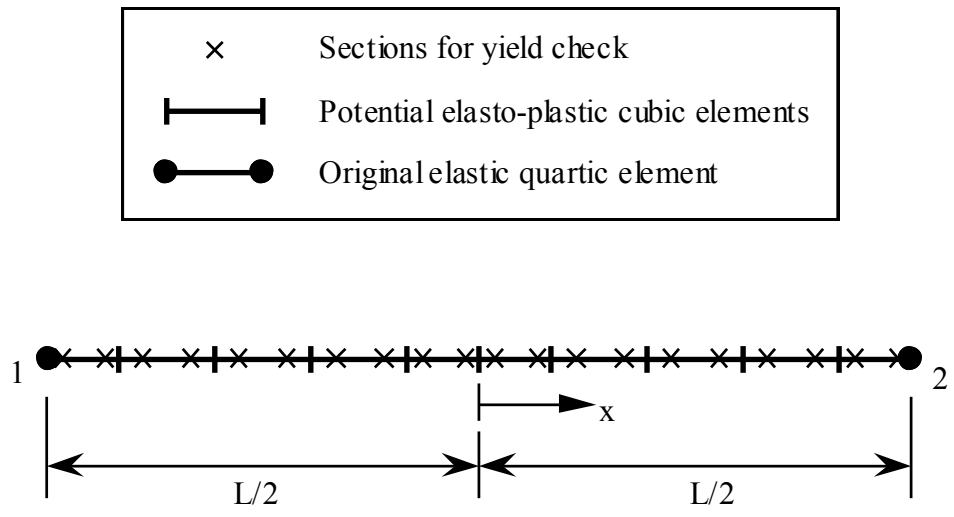


Figure 5. An example configuration for a refined mesh

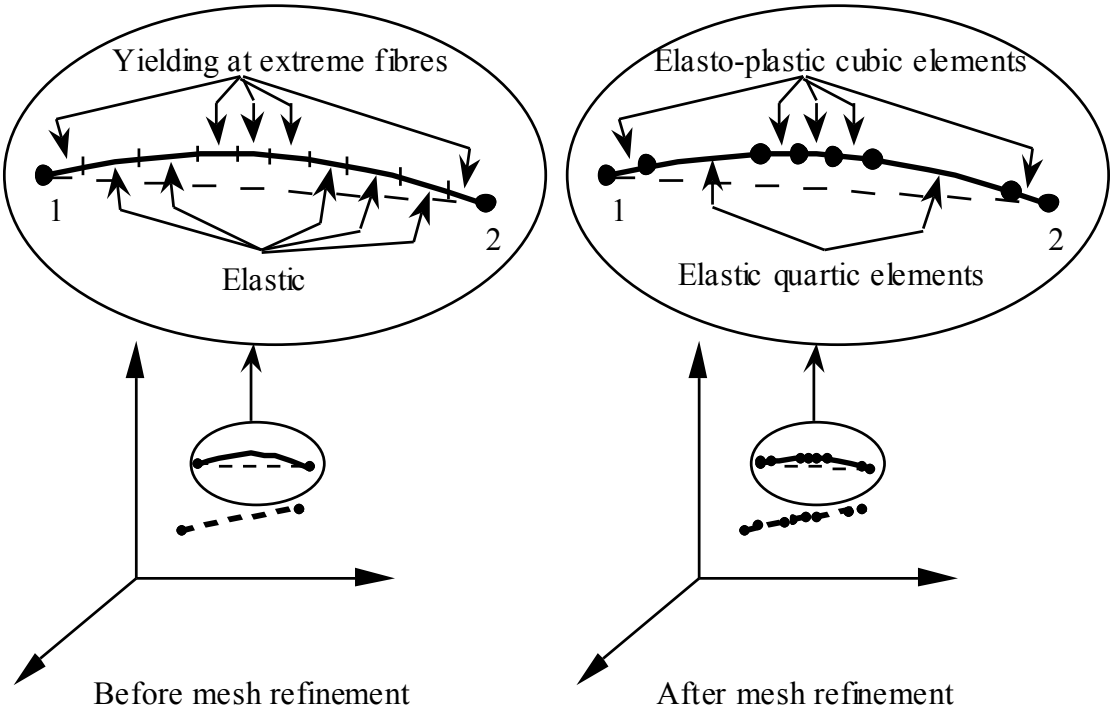


Figure 6. Mesh refinement of quartic element

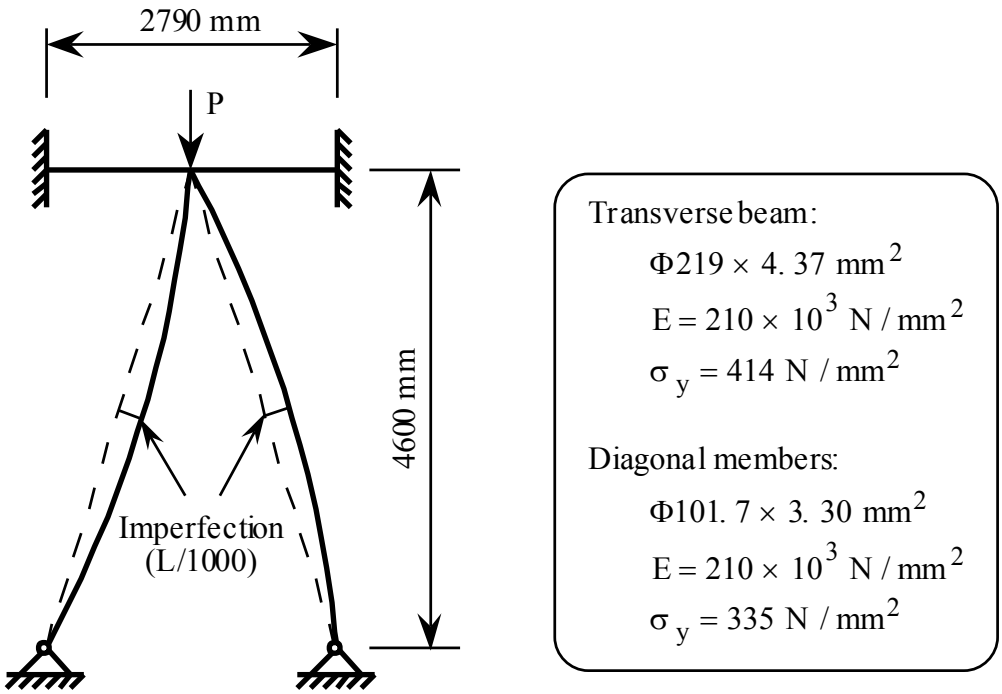


Figure 7. Geometric configuration of K-frame

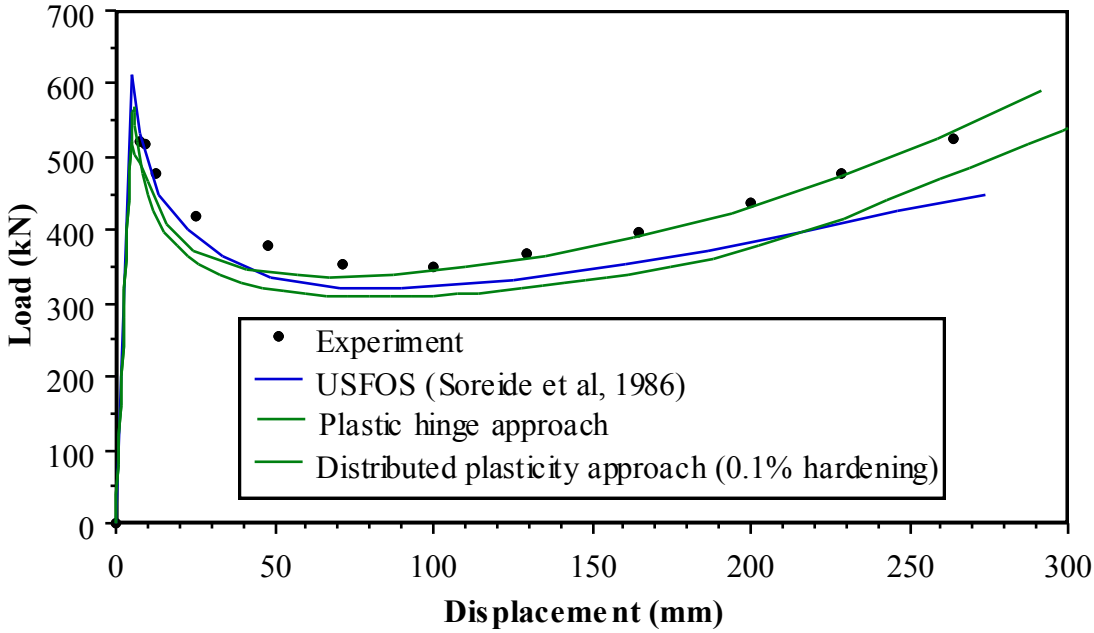


Figure 8. Static response of K-frame

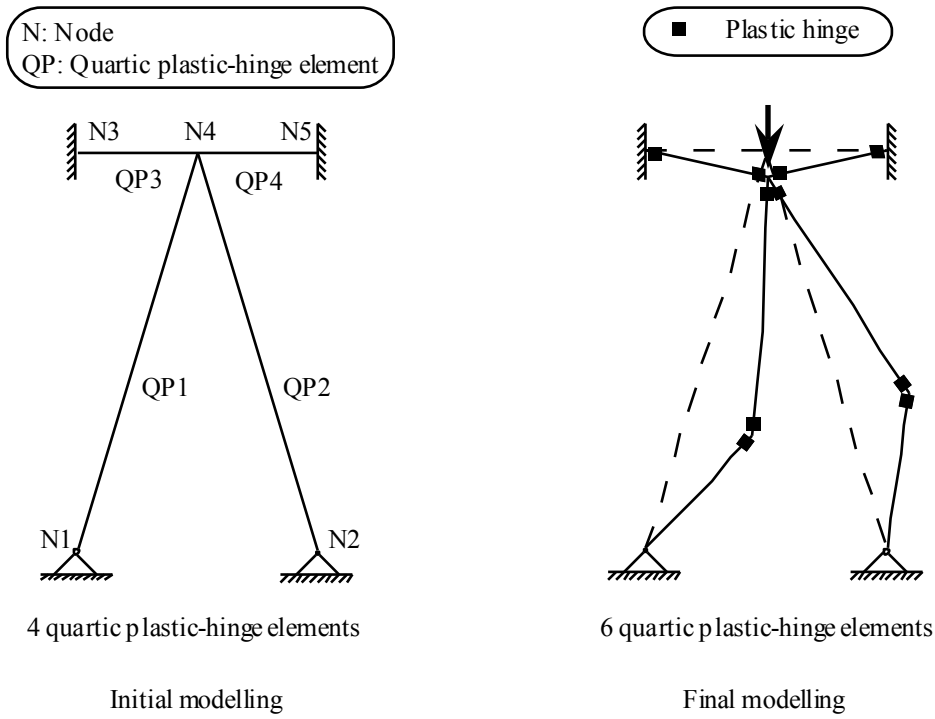


Figure 9. Modelling of K-frame with the plastic hinge approach

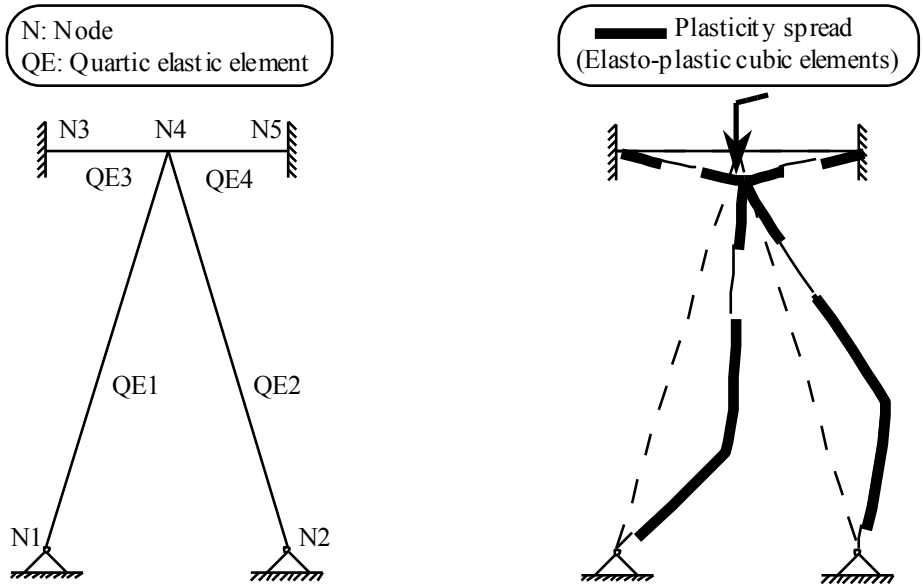


Figure 10. Modelling of K-frame with the distributed plasticity approach

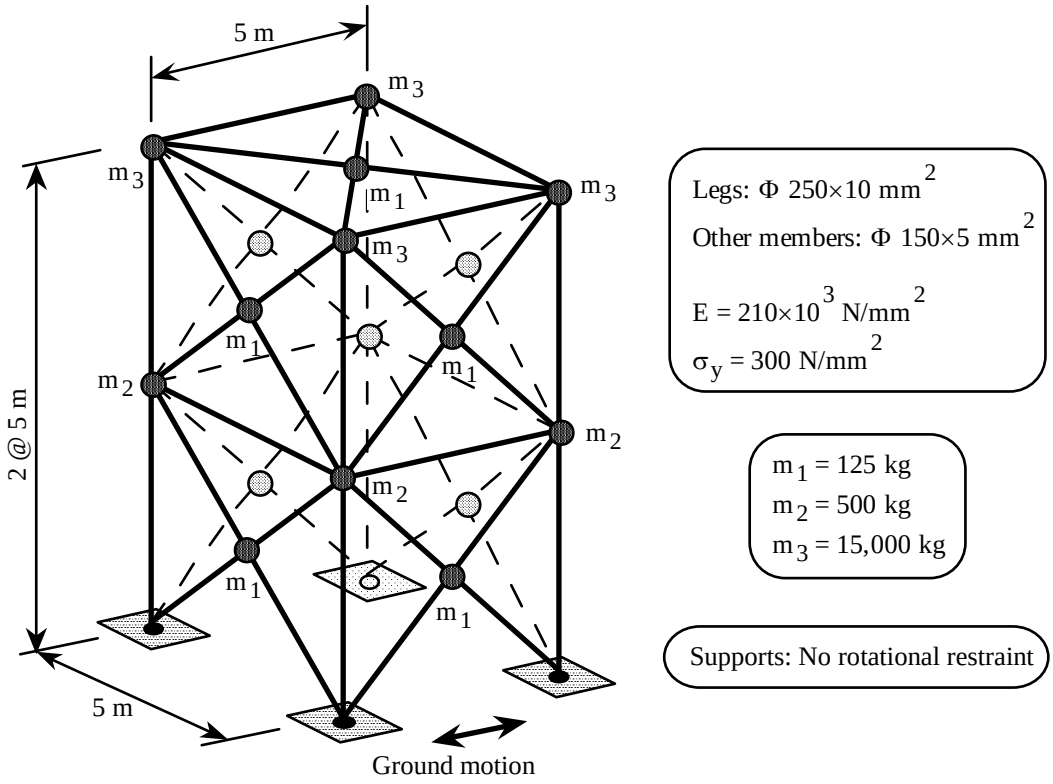


Figure 11. Geometric configuration of one-bay steel jacket

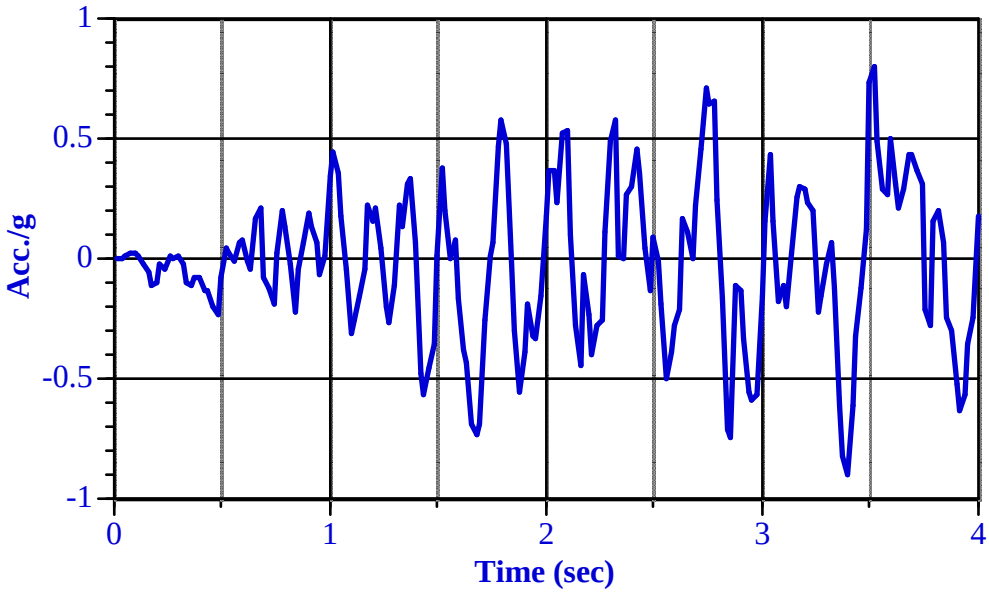


Figure 12. Transient signal applied to steel jacket

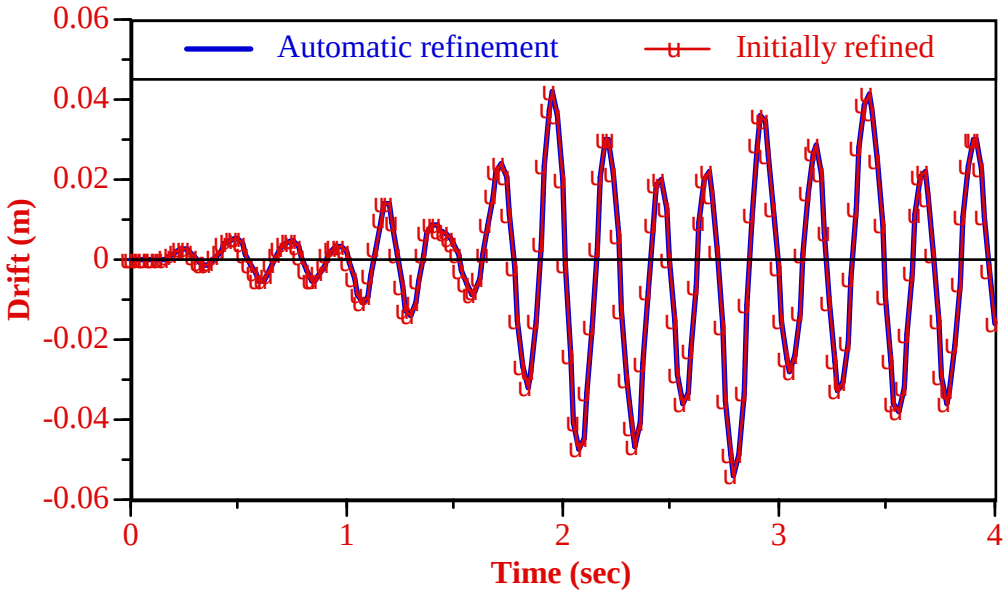
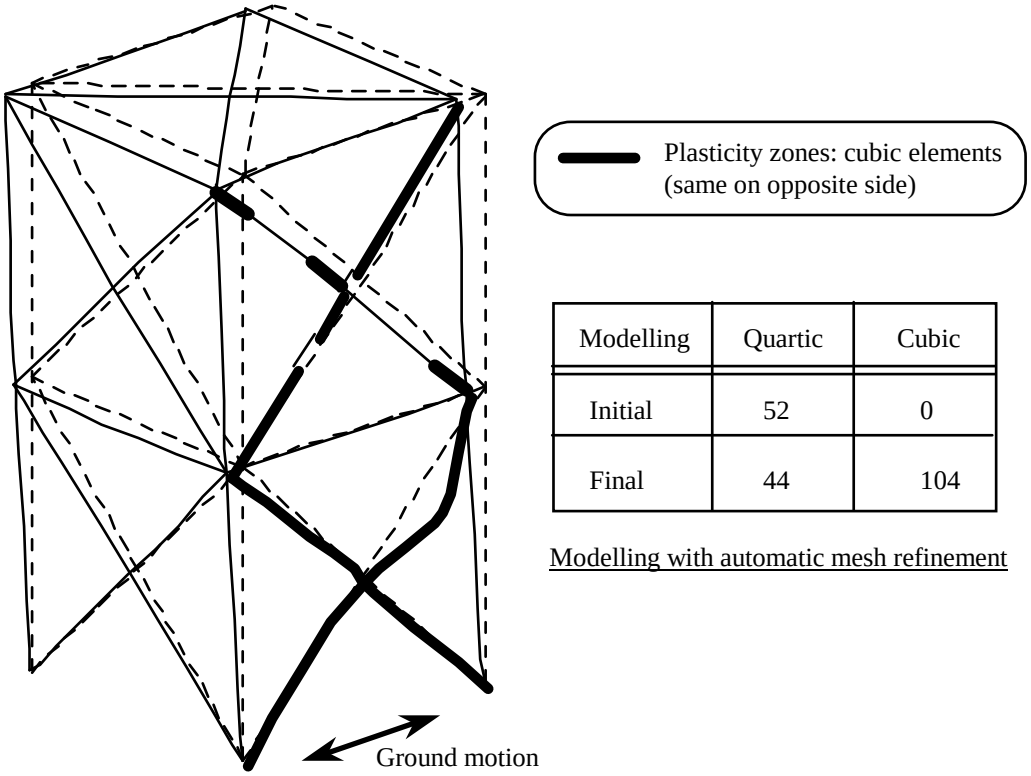


Figure 13. Response of steel jacket to transient signal



Modelling	Quartic	Cubic
Initial	52	0
Final	44	104

Modelling with automatic mesh refinement

Figure 14. Deflected shape of steel jacket

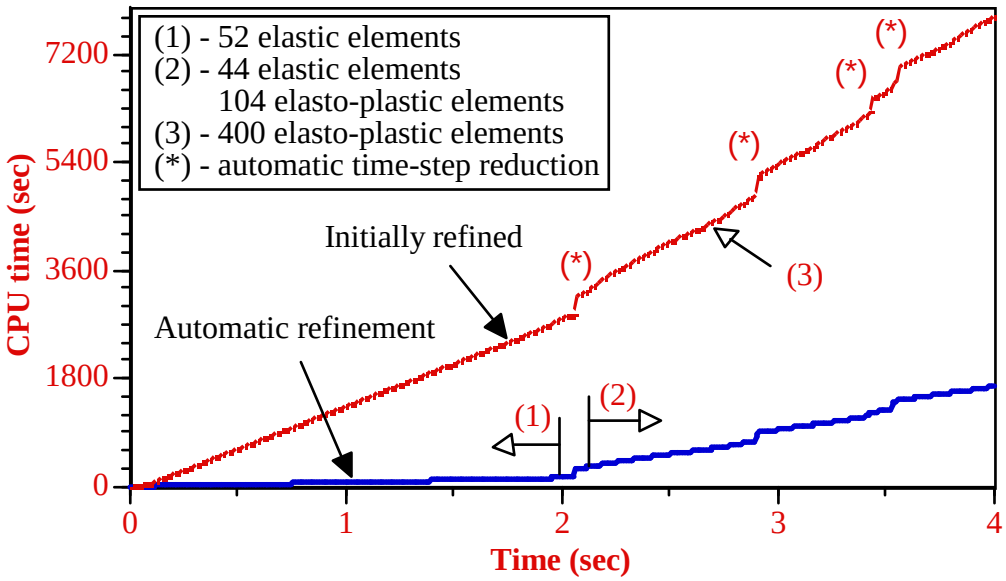


Figure 15. CPU time for analysis of steel jacket

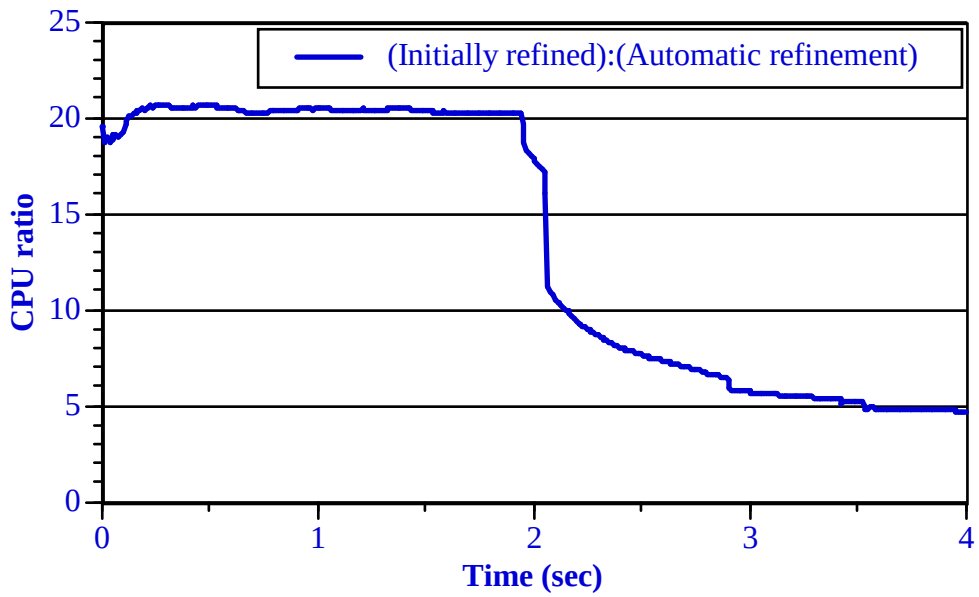


Figure 16. CPU savings with automatic mesh refinement

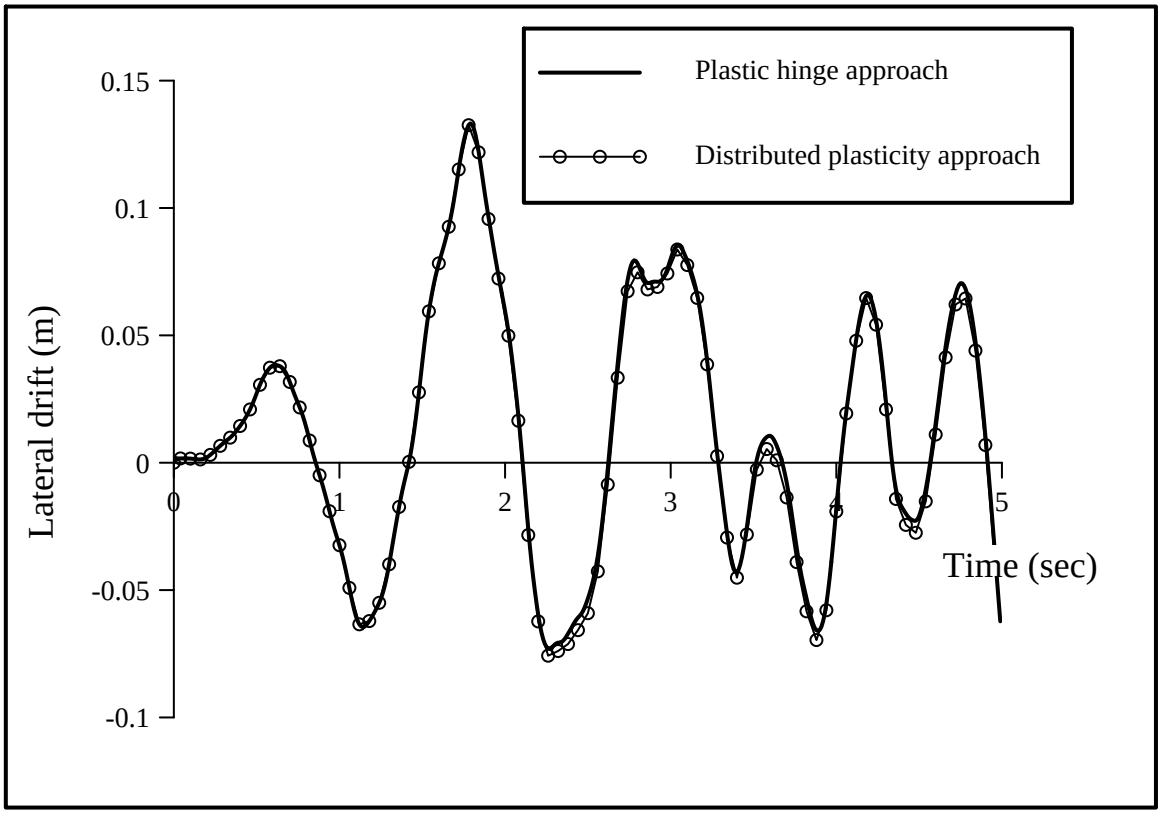


Figure 17. Response of three-dimensional jacket to earthquake signal

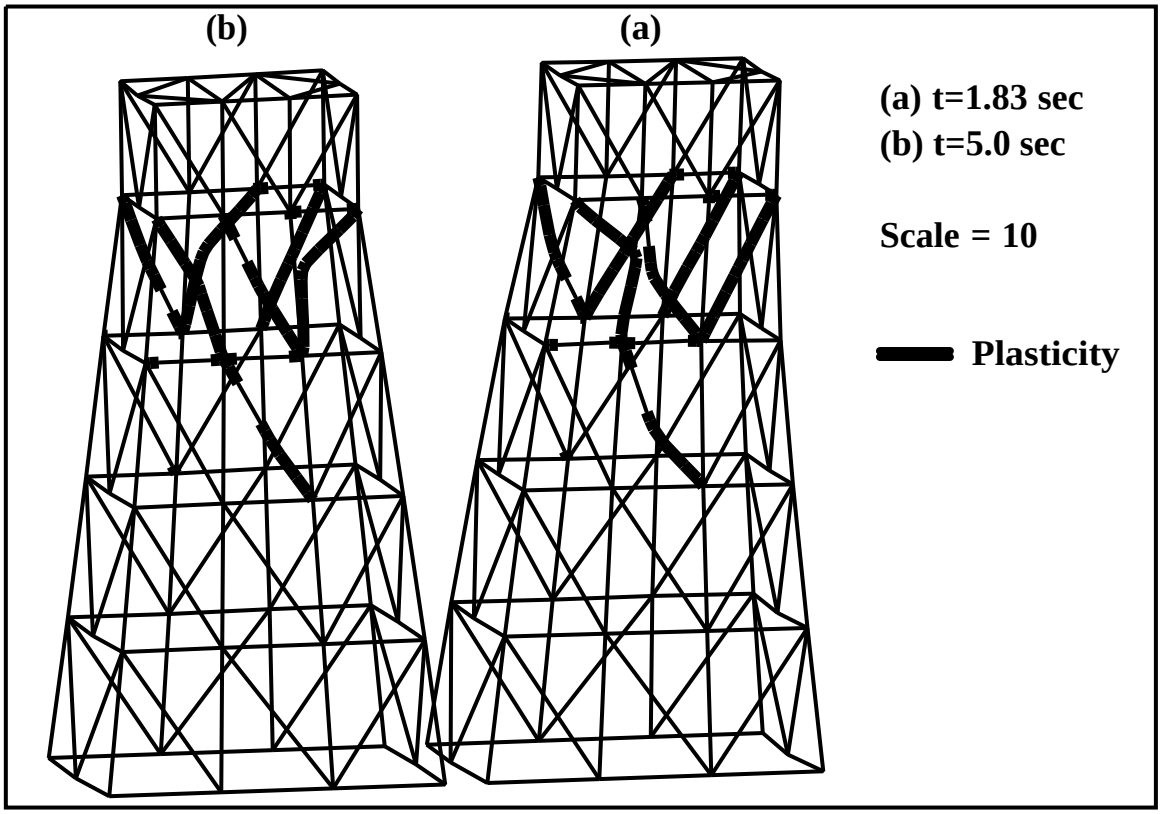


Figure 18. Deflected shape of three-dimensional jacket